IOSR Journal of Mechanical and Civil Engineering (IOSR-JMCE)
e-ISSN: 2278-1684,p-ISSN: 2320-334X, Volume 15, Issue 3 Ver. IV (May. - June. 2018), PP 59-76
www.iosrjournals.org

Vibration analysis of orthotropic double-nanoplate system subjected to unidirectional in-plane magnetic field with various boundary conditions

Nebojša Radić[1], Dejan Jeremić[2], Biljana Mijatović[3]
Department of Applied Mechanics, Faculty of Mechanical Engineering/ University of East Sarajevo, Bosnia and Herzegovina
Corresponding author: Nebojša Radić

Abstract: *The present study investigates the vibration behaviour of orthotropic double-nanoplate system subjected to an in-plane magnetic field and in-plane preload with various boundary conditions. The nonlocal governing equations of motion are derived via Hamilton's principle with the consideration the Eringen's differential nonlocal elastic law, where the influences of the Lorenz magnetic force are obtained via a Maxwell's relation. Analytical methods are employed and explicit solutions for vibrational frequency are obtained for orthotropic double-nanoplate system for various boundary conditions. The obtained results are compared with the results available in the literature to check their validation. Effects of nonlocal parameter, magnetic field strength, number of half waves, initial preload (compression and tension), size of nanoplate and boundary conditions on vibrational frequency are presented.*

Date of Submission: 13-06-2018 Date of acceptance: 30-06-2018

I. Introduction

Nanostructural elements, among which the best-known ones are carbon nanotube (CNT) and graphene sheet (GS), due to their extraordinary physical, chemical and mechanical properties can have a wide possible application in nanoelectro-mechanical systems (NEMS) as mechanical sensors[1], biosensors[2], nanoactuators[3] and nanoresonators[4]. Besides that, CNT and GS have a great perspective to be applied in medicine, astronautics and energy storage systems. Due to their extraordinary mechanical properties, GS can be used as excellent reinforcement of polymer composites. Regarding the fact that CNT presents a deformed form of GS it can be concluded that for a successful development of carbon-based nanostructures it is very importance to know accurately the physical, mechanical and electrical features of GS. Besides that, for a successful application of GS as a nanostructural component and a nanomaterial it is very important to know its vibrational behaviour. Both experimental and molecular dynamic simulation (MD simulation) show that in nanostructural elements with very small dimensions their mechanical properties and behaviour change when these dimensions become very small. However, the classical elasticity theory cannot take into account the size effect in the analysis of mechanical behaviour of micro- and nanostructures.

Due to very small dimensions of nanoplates, it is necessary to take into account the influence of atomic forces to their mechanical behaviour. It is known that the influence of atomic forces has been neglected in classical elasticity theory. However, in the first papers which discussed the vibrational behaviour of graphene sheet classical elasticity theory[5,6,7,8] was used. Arash and Wang[9] demonstrated that by the application of classical elasticity theory significantly higher values were obtained for the resonant frequency then its real value. The application of MD simulation is too complex and expensive, especially in the case of more complex nanostructures with a greater number of atoms. Because of that, a few classical continuum theories have been developed in which the small-scale size effect has been incorporated into constitutive equations and governing equations of motion/equilibrium. There belong the nonlocal elasticity theory[10,11,12,13], strain gradient theory[14,15] and couple stress theory[16,17]. Due to its relatively simple formulation and applicability, in recent years the nonlocal elasticity theory has been widely applied in the defining of nonlocal governing equations of motion/equilibrium of nanostructures. Pradhan and Kumar [18] examined the nonlocal influences on the vibrational behaviour of the orthotropic graphene sheets using nonlocal elasticity theory and differential quadrature method.

The effect of in-plane preload on vibrations of nanoplate via nonlocal elasticity was investigated by Murmu and Pradhan[19]. Kiani[20] applied the nonlocal shear deformation theory to investigate the vibration of double-walled carbon nanotubes on elastic foundation subjected to axial preload. Mohammadi et al.[21] investigated the free vibration behaviour of circular graphene sheet under in-plane preload using nonlocal

continuum theory. In recent time, double-layered nanoplate structures have been in the focus of research more. Asemi et al.[22] studied the vibration behaviour of double-piezoelectric-nanoplate with initial stress under an external electric voltage and various boundary conditions using differential quadrature method. Mohammadimehr et al.[23] carried out the free vibration analysis of viscoelastic double layered nanoplates using sinusoidal shear deformation theory and meshless method. Liu et.al[24] presented the nonlocal vibration and biaxial buckling behaviour of simply supported double-viscoelastic-FGM-nanoplate system with viscoelastic medium in between. Radić and Jeremić[25] formulated the new first order shear deformation theory via nonlocal elasticity theory for analysing the thermal buckling of isotropic double-layered graphene sheets with various boundary conditions. Radić and Jeremić[26] researched the nonlocal vibration and buckling of orthotropic double-layered graphene sheets with different boundary conditions subjected to hygrothermal loading using nonlocal elasticity theory and Galerkin's method. When a nanostructure is exposed to the activity of magnetic field, then, as the consequence of the activity, Lorentz's forces occur, which are the body forces and act to every elementary particle of that structure. In the absence of experimental research on the influence of Lorentz's forces to the vibration and buckling behaviour of nanoplates, a great significance is given to the theoretical research based on Maxwell's equations.

Güven[27] studied the effects of longitudinal magnetic field and initial stress on the transverse vibration of single-walled carbon nanotubes. Kiani[28] scrutinized free transverse vibrations of double-walled carbon nanotubes subjected to a longitudinally varying magnetic field with various boundary conditions. Murmu et al.[29] examined vibration behaviour of double-walled carbon nanotubes subjected to a longitudinal magnetic field using a nonlocal Euler-Bernoulli beam theory. Kiani3[0] investigated the vibration and instability of a single-walled carbon nanotube in a three-dimensional magnetic field using nonlocal Rayleigh beam theory. Transverse vibration behaviour of embedded single-layer graphene sheets exposed to in-plane magnetic field with simply supported boundary conditions is analysed by Murmu et al.[31] . Kiani[32] presented free vibration behaviour of single-layer nanoplates subjected to in-plane magnetic field with simply supported boundary conditions using nonlocal shear deformable plate theories. Vibration behaviour of double bonded orthotropic graphene sheets subjected to 2D magnetic field and biaxial in-plane preload using differential quadrature method was investigated by Ghorbanpour Arani et al[33]. In other works, the nonlocal vibrations of axially moving graphene sheet resting on orthotropic visco-Pasternak foundation under longitudinal magnetic field using the hybrid analytical-numerical method for solution were addressed by Ghorbanpour Arani et al[34]. Vibration analysis of bilayer graphene sheets subjected to in-plane magnetic field using nonlocal elasticity theory and nonlocal element-free kp-Ritz method has been studied by Zhang et al.[35] .Karličić et al.[36] investigated the nonlocal vibration of multi-nanoplate system embedded in viscoelastic medium under in-plane magnetic field. Stamenković Atanasov et al.[37] expressed the influence of an in-plane magnetic field on the forced transverse vibration of orthotropic double-nanoplate system with simply supported boundary conditions using Kirchhof-Love plate theory. Satish et al.[38] studied the thermal vibration of single-layer nanoplates subjected to in-plane magnetic field and surface elasticity effects with simply supported boundary conditions using Navier's method for solution. Jamalpoor and Hosseini[39] presented the in-plane magnetic field effects on biaxial buckling of simply supported double-orthotropic micro-plate-systems using nonlocal strain gradient theory.

Ebrahimi and Reza Barati[40] investigated the vibration of graphene sheets subjected to hygro-thermal and in-plane magnetic field based on the nonlocal strain gradient theory. Shimpi et al.[41] formulated new-first order shear deformation theory (NFSDT) and showed that it has been significantly more accurate then classical plate theory (CLPT) with very few deviations from first-shear deformation theory (FSDT) for isotropic and orthotropic rectangular plate with symmetric boundary conditions. Xian and Xing[42] studied free vibrations of rectangular plates with various boundary conditions using the NFSDT. Thai et al.[43] investigated the bending, buckling and free vibration of functionally graded sandwich plates with different boundary conditions via the NFSDT. A verification study showed that the NFSDT was more accurate in relation FSDT and comparable to higher-order shear deformation theory (HSDT). Radić and Jeremić[25] formulated the solution for the nonlocal vibration of isotropic DLGSs using the nonlocal formulation of the NFSDT. The verification study in Refs.[25,26] showed that the nonlocal NFSDT could be applied very successfully in the analysis of buckling and vibration behaviour of isotropic and orthotropic nanoplates. The advantage of the NFSDT in relation to FSDT can be seen in the fact that we have only one parameter of rotation instead of two, so it can be said that the NFSDT is a reduced version of the FSDT. A drawback of the NFSDT is in the fact that it cannot be used in the analysis of anisotropic nanostructures, and in the analysis of asymmetrical boundary conditions the results may be obtained which are not accurate enough. To the best author's knowledge transverse vibration analysis of the orthotropic DLGSs subjected to in-plane magnetic and initial in-plane preload with various boundary conditions has not been covered using nonlocal continuum mechanics until now. In the present paper, using differential nonlocal elastic law we study the influence of a unidirectional in-plane magnetic field and initial in-plane preload on the vibration behaviour of DLGS. The governing equations of motion are derived based on new first-order shear deformation theory (NFSDT), Eringen's differential nonlocal elastic law and the Hamilton's principle.

Analytical solution for frequency is based on functions which satisfy different boundary conditions. The effects of nonlocal parameter, magnetic field strength, in-plane preload, boundary conditions, aspect ratio, side length and number of half waves on the vibration behaviour of DLGSs are examined.

II. Problem formulation

A schematic configuration of the orthotropic DLGS which consists of two layers of graphene sheets (GS_1 and GS_2), with length a, width b and thickness h embedded in Pasternak foundation subjected to in-plane magnetic field H_x has been illustrated in Fig.1.

Fifure no 1: Geometry, coordinate system and loading for orthotropic double-layered graphene sheet

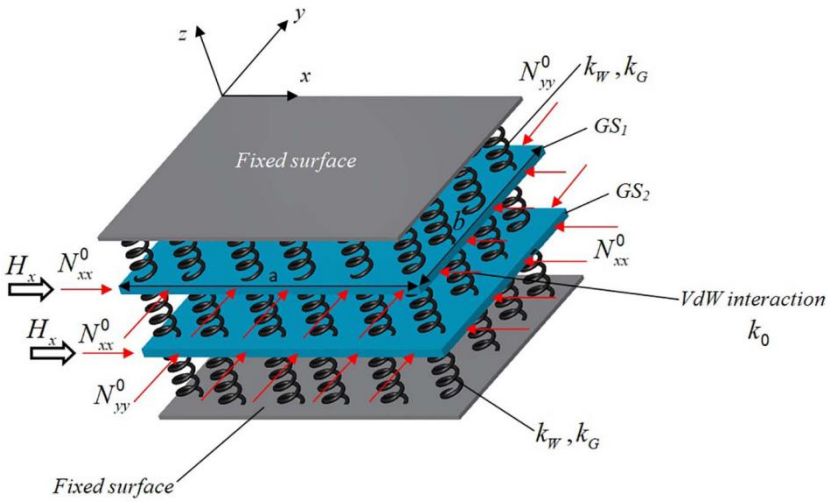

GS_1 and GS_2 are in the interaction by van der Waals (vdW) interaction forces shown by a set of springs with modulus k_0. As it can be seen, two sheets are surrounded by an external Pasternak elastic medium, where k_w and k_G are Winkler modulus parameter and shear modulus parameter respectively. As depicted N^0_{xx} and N^0_{yy} denote two uniform preload forces in the x and y directions. The material characteristics used for both graphene sheets are identical.

The new first-order shear deformation theory (NFSDT)

According to the new first-order shear deformation theory, the displacement field of the graphene sheet is expressed by

$$\begin{aligned} u_x(x,y,z) &= u(x,y) - z\frac{\partial \phi}{\partial x} \\ u_y(x,y,z) &= v(x,y) - z\frac{\partial \phi}{\partial y} \\ u_z(x,y,z) &= w(x,y) \end{aligned} \tag{1}$$

where u and v are the displacement of mid-plane along x- and y-axis respectively, w is transverse displacement of a point on the mid-plane of the graphene sheet, and ϕ is rotation parameter.

Nonzero strains of the NFSDT model are expressed as

$$\begin{Bmatrix} \varepsilon_{xx} \\ \varepsilon_{yy} \\ \varepsilon_{xy} \end{Bmatrix} = \begin{Bmatrix} \dfrac{\partial u}{\partial x} \\ \dfrac{\partial v}{\partial y} \\ \dfrac{\partial u}{\partial y} + \dfrac{\partial v}{\partial x} \end{Bmatrix} - z \begin{Bmatrix} \dfrac{\partial^2 \phi}{\partial x^2} \\ \dfrac{\partial^2 \phi}{\partial y^2} \\ 2\dfrac{\partial^2 \phi}{\partial x \partial y} \end{Bmatrix}, \quad \begin{Bmatrix} \varepsilon_{yz} \\ \varepsilon_{xz} \end{Bmatrix} = \begin{Bmatrix} \dfrac{\partial w}{\partial y} - \dfrac{\partial \phi}{\partial y} \\ \dfrac{\partial w}{\partial x} - \dfrac{\partial \phi}{\partial x} \end{Bmatrix} \tag{2}$$

Nonlocal constitutive equations

According to nonlocal differential elastic law by Eringen[10,11], the nonlocal stress tensor at a reference point x in an elastic continuum depends not only on strain tensor at that point but also on the strain tensor at all

other points x' on the observed domain. The strain-driven integral constitutive equation for a linear, homogeneous, orthotropic, nonlocal elastic body neglecting the body forces can be expressed as

$$t_{ij}(x) = \int_V \alpha(|x'-x|,\xi)\sigma_{ij}(x')dV(x') \quad i,j = x,y,z \tag{3}$$

where $t_{ij}(x)$ and $\sigma_{ij}(x')$ are respectively, the nonlocal stress tensor and classical or local stress tensor at any point x' in the body, nonlocal kernel function $\alpha(|x'-x|,\xi)$ represents the nonlocal module and it defines the influence of deformation in the point x' to the stress in the observed point x, $\xi = e_0\ell / \ell_e$ is a material constant that depends on the internal characteristic length ℓ (e.g. lattice parameter, granular size, or molecular diameters) and external characteristic length ℓ_e (e.g. crack length, wave length), e_0 is the constant appropriate to each material and it is determined independently for each material, on the basis of experimental results or other theories. Local stress tensor at a point x' can be expressed vie the deformation tensor by the generalized Hook's law

$$\sigma_{ij}(x') = C_{ijkl}\varepsilon_{kl}(x') \qquad i,j,k,l = x,y,z \tag{4}$$

where C_{ijkl} is the fourth-order elasticity tensor and $\varepsilon_{kl}(x')$ is the strain tensor

The strain-driven integral constitutive equation (3) is very difficult to apply. Making certain assumptions presented by Eringen [10,11] we will assume the consequent (not equivalent) differential constitutive laws as

$$\left[1-(e_0\ell)^2\nabla^2\right]t_{ij}(x) = C_{ijkl}\varepsilon_{kl} \quad i,j,k,l = x,y,z \tag{5}$$

where ∇^2 is the Laplacian operator which is defined by $\nabla^2 = (\partial^2/\partial x^2 + \partial^2/\partial y^2)$,and $e_0\ell$ is the nonlocal parameter that takes into account the small scale effects into the differential constitutive law.

Maxwell's relations

In this section we present Maxwell's relations. Denoting $\vec{J}$ as current density, $\vec{U}$ as the displacement vector, η as magnetic field permeability, $\vec{e}$ as strength vector of magnetic field and $\vec{h}$ is disturbing vectors of magnetic field, the Maxwell's relations of electromagnetics according to[29,46] are given as

$$\vec{J} = \nabla\times\vec{h},\ \nabla\times\vec{e} = -\eta\frac{\partial\vec{h}}{\partial t},\ \nabla\cdot\vec{h} = 0,\ \vec{e} = -\eta\left(\frac{\partial\vec{U}}{\partial t}\times\vec{H}\right),\ \vec{h} = \nabla\times\left(\vec{U}\times\vec{H}\right) \tag{6}$$

where ∇ is the Hamilton operator and is expressed as $\nabla = \frac{\partial}{\partial x}\vec{i} + \frac{\partial}{\partial y}\vec{j} + \frac{\partial}{\partial z}\vec{k}$. Consider the magnetic field vector as $\vec{H} = (H_x, H_y, H_z)$, which exerted on the DLGSs. Let the displacement vector be $\vec{U} = (u_x, u_y, u_z)$, then

$$\begin{aligned}\vec{h} = \nabla\times(\vec{U}\times\vec{H}) &= \left(\frac{\partial u_x}{\partial y}H_y - \frac{\partial u_y}{\partial y}H_x - \frac{\partial u_z}{\partial z}H_x + \frac{\partial u_x}{\partial z}H_z\right)\vec{i} \\ &+\left(\frac{\partial u_y}{\partial z}H_z - \frac{\partial u_z}{\partial z}H_y - \frac{\partial u_x}{\partial x}H_y + \frac{\partial u_y}{\partial x}H_x\right)\vec{j} + \left(\frac{\partial u_z}{\partial x}H_x - \frac{\partial u_x}{\partial x}H_z - \frac{\partial u_y}{\partial y}H_z + \frac{\partial u_z}{\partial y}H_y\right)\vec{k}\end{aligned} \tag{7}$$

$$\vec{J} = \nabla\times\vec{h} = J_x\vec{i} + J_y\vec{j} + J_z\vec{k} \tag{8}$$

where

$$
\begin{aligned}
J_x &= \frac{\partial^2 u_z}{\partial x \partial y} H_x - \frac{\partial^2 u_x}{\partial x \partial y} H_z - \frac{\partial^2 u_y}{\partial y^2} H_z + \frac{\partial^2 u_z}{\partial y^2} H_y - \frac{\partial^2 u_y}{\partial z^2} H_z + \frac{\partial^2 u_z}{\partial z^2} H_y \\
&\quad + \frac{\partial^2 u_x}{\partial x \partial z} H_y - \frac{\partial^2 u_y}{\partial x \partial z} H_x \\
J_y &= \frac{\partial^2 u_x}{\partial y \partial z} H_y - \frac{\partial^2 u_y}{\partial y \partial z} H_x - \frac{\partial^2 u_z}{\partial z^2} H_x + \frac{\partial^2 u_x}{\partial z^2} H_z - \frac{\partial^2 u_z}{\partial x^2} H_x + \frac{\partial^2 u_x}{\partial x^2} H_z \\
&\quad + \frac{\partial^2 u_y}{\partial x \partial y} H_z - \frac{\partial^2 u_z}{\partial x \partial y} H_y \\
J_z &= \frac{\partial^2 u_y}{\partial x \partial z} H_z - \frac{\partial^2 u_z}{\partial x \partial z} H_y - \frac{\partial^2 u_x}{\partial x^2} H_y + \frac{\partial^2 u_y}{\partial x^2} H_x - \frac{\partial^2 u_x}{\partial y^2} H_y + \frac{\partial^2 u_y}{\partial y^2} H_x \\
&\quad + \frac{\partial^2 u_z}{\partial y \partial z} H_x - \frac{\partial^2 u_x}{\partial y \partial z} H_z
\end{aligned}
\tag{9}
$$

The Lorenz force induced by magnetic field is

$$
\begin{aligned}
&\vec{f} = f_x \vec{i} + f_y \vec{j} + f_z \vec{k} = \eta(\vec{J} \times \vec{H}) \\
&= \eta\left[\left(J_y H_z - J_z H_y\right)\vec{i} + \left(J_z H_x - J_x H_z\right)\vec{j} + \left(J_x H_y - J_y H_x\right)\vec{k}\right]
\end{aligned}
\tag{10}
$$

In the present paper, we consider a uniaxial magnetic field. Therefore, the Lorentz force components along the *x, y* and *z* direction, induced by the uniaxial in-plane magnetic field H_x is given as

$$f_x = 0 \tag{11a}$$

$$f_y = \eta H_x^2 \left(\frac{\partial^2 u_y}{\partial x^2} + \frac{\partial^2 u_y}{\partial y^2} + \frac{\partial^2 u_z}{\partial y \partial z} \right) = \eta H_x^2 \left(\frac{\partial^2 v}{\partial x^2} + \frac{\partial^2 v}{\partial y^2} - z \frac{\partial^3 \phi}{\partial^2 x \partial y} - z \frac{\partial^3 \phi}{\partial y^3} \right) \tag{11b}$$

$$f_z = \eta H_x^2 \left(\frac{\partial^2 u_z}{\partial x^2} + \frac{\partial^2 u_z}{\partial z^2} + \frac{\partial^2 u_y}{\partial y \partial z} \right) = \eta H_x^2 \left(\frac{\partial^2 w}{\partial x^2} - \frac{\partial^2 \phi}{\partial y^2} \right) \tag{11c}$$

The effective Lorenz forces in the direction of y and z axis can be written as

$$F_y = \int_{-h/2}^{h/2} f_y dz = \eta h H_x^2 \left(\frac{\partial^2 v}{\partial x^2} + \frac{\partial^2 v}{\partial y^2} \right) \tag{12a}$$

$$F_z = \int_{-h/2}^{h/2} f_z dz = \eta h H_x^2 \left(\frac{\partial^2 w}{\partial x^2} - \frac{\partial^2 \phi}{\partial y^2} \right) \tag{12b}$$

In this study only the transverse vibrations of the DLGS are significant. According to (12a) it is obvious that the transverse and in-plane vibration are not related. Also, because of the very low thickness of the nanoplate $(h = 0.34\,nm)$ as in Ref.[46] we will neglect the value of the bending moment

$$M_{yy} = \int_{-h/2}^{h/2} z f_y dz = -\frac{\eta h^3 H_x^2}{12} \left(\frac{\partial^3 \phi}{\partial x^2 \partial y} + \frac{\partial^3 \phi}{\partial y^3} \right)$$

Nonlocal governing equations of motion

Based on Eqs. (2) and (5) the stress-strain equations of a rectangular orthotropic graphene sheet are expressed as follows:

$$\begin{Bmatrix}\sigma_{xx}\\ \sigma_{yy}\\ \sigma_{xy}\\ \sigma_{yz}\\ \sigma_{zx}\end{Bmatrix}-(e_0\ell)^2\nabla^2\begin{Bmatrix}\sigma_{xx}\\ \sigma_{yy}\\ \sigma_{xy}\\ \sigma_{yz}\\ \sigma_{zx}\end{Bmatrix}=\begin{Bmatrix}Q_{11} & Q_{12} & 0 & 0 & 0\\ Q_{21} & Q_{22} & 0 & 0 & 0\\ 0 & 0 & Q_{66} & 0 & 0\\ 0 & 0 & 0 & C_{44} & 0\\ 0 & 0 & 0 & 0 & C_{55}\end{Bmatrix}\begin{Bmatrix}\varepsilon_{xx}\\ \varepsilon_{yy}\\ \varepsilon_{xy}\\ \varepsilon_{yz}\\ \varepsilon_{zx}\end{Bmatrix} \tag{13}$$

where Q_{ij} and C_{ij} are stiffness of the orthotropic layer graphene sheet defined by

$$Q_{11}=\frac{E_1}{1-\nu_{12}\nu_{21}},\ Q_{12}=\frac{\nu_{12}E_2}{1-\nu_{12}\nu_{21}}=Q_{21}=\frac{\nu_{21}E_1}{1-\nu_{12}\nu_{21}},\ Q_{22}=\frac{E_2}{1-\nu_{12}\nu_{21}},$$
$$Q_{66}=G_{12}, C_{44}=G_{23},\ C_{55}=G_{31} \tag{14}$$

where E_1 and E_2 are Young's moduli in directions *x* and *y*, respectively, G_{12}, G_{13}, G_{23} are shear modulus and ν_{12}, ν_{21} denote Poisson's ratios.

The nonlocal stress resultants M_i and Q_j for orthotropic graphene sheet are expressed as

$$M_i=\int_{-h/2}^{h/2} z\sigma_i dz$$
$$Q_j=K_S\int_{-h/2}^{h/2}\sigma_j dz\quad (i=xx,yy,xy;\ j=yz,zx) \tag{15}$$

In which $K_s=5/6$ is the transverse shear correction factor. By substituting Eqs. (2) and (13) into Eq. (15), the nonlocal constitutive equations in terms of displacement are obtained

$$M_{xx}-(e_0\ell)^2\nabla^2 M_{xx}=-\left[D_{11}\frac{\partial^2\phi}{\partial x^2}+D_{12}\frac{\partial^2\phi}{\partial y^2}\right]$$
$$M_{yy}-(e_0\ell)^2\nabla^2 M_{yy}=-\left[D_{22}\frac{\partial^2\phi}{\partial y^2}+D_{12}\frac{\partial^2\phi}{\partial x^2}\right] \tag{16}$$
$$M_{xy}-(e_0\ell)^2\nabla^2 M_{xy}=-2D_{66}\frac{\partial^2\phi}{\partial x\partial y}$$

$$Q_{xz}-(e_0\ell)^2\nabla^2 Q_{xz}=H_{55}\left(\frac{\partial w}{\partial x}-\frac{\partial\phi}{\partial x}\right)$$
$$Q_{yz}-(e_0\ell)^2\nabla^2 Q_{yz}=H_{44}\left(\frac{\partial w}{\partial y}-\frac{\partial\phi}{\partial y}\right) \tag{17}$$

where $D_{ij}(i,j=1,2,6)$ and H_{44}, H_{55} are the bending and shear stiffness of the graphene sheet defined by

$$D_{11}=\frac{Q_{11}h^3}{12},\quad D_{22}=\frac{Q_{22}h^3}{12},\quad D_{12}=\frac{Q_{12}h^3}{12},\quad D_{66}=\frac{Q_{66}h^3}{12},$$
$$H_{44}=K_S C_{44}h,\quad H_{55}=K_S C_{55}h, \tag{18}$$

To obtain the nonlocal equations of motion of DLGSs, the Hamilton's principle is expressed as:

$$\int_0^t \delta(U+V-T)dt=0 \tag{19}$$

In which *U* is the strain energy, *V* is the work done by external loads and *T* is the kinetic energy. The two graphene sheet are referred as GS_1 and GS_2. The transverse displacements of GS_1 and GS_2 are assumed w_1 and w_2 respectively.

The variation of strain energy is calculated as

$$\delta U = \int_{-h/2}^{h/2}\int_{A}\sigma_{ij1}\delta\varepsilon_{ij1}dAdz = \int_{-h/2}^{h/2}\int_{A}(\sigma_{xx1}\delta\varepsilon_{xx1}+\sigma_{yy1}\delta\varepsilon_{yy1}+\sigma_{xy1}\delta\varepsilon_{xy1}+\sigma_{yz1}\delta\varepsilon_{yz1}+\sigma_{xz1}\delta\varepsilon_{xz1})dAdz \tag{20}$$

Substituting Eqs. (2) into Eq. (20) yields

$$\delta U = \int_{A}\Bigg[N_{xx}\frac{\partial\delta u_1}{\partial x} - M_{xx}\frac{\partial^2\delta\phi_1}{\partial x^2} + N_{yy}\frac{\partial\delta v_1}{\partial y} - M_{yy}\frac{\partial^2\delta\phi_1}{\partial y^2} + \\ + N_{xy}\left(\frac{\partial\delta u_1}{\partial y}+\frac{\partial\delta v_1}{\partial x}\right) - 2M_{xy}\frac{\partial^2\delta\phi_1}{\partial x\partial y} + Q_{xz}\frac{\partial\delta\left(w_1-\phi_1\right)}{\partial x} + Q_{yz}\frac{\partial\delta\left(w_1-\phi_1\right)}{\partial y}\Bigg] \tag{21}$$

Where the index 1 marks for displacements indicates that graphene sheets 1 is in question. The term f_z is the consequence of activity to the in-plane magnetic field H_x.The effective transverse Lorentz magnetic load for graphene sheet 1 (GS_1) is obtained as

$$q_{1magnetic} = \int_{-h/2}^{h/2} f_{z1}dz = hf_{z1} = \eta hH_x^2\left(\frac{\partial^2 w_1}{\partial x^2}-\frac{\partial^2\phi_1}{\partial y^2}\right) \tag{22}$$

The effective transverse load of Pasternak elastic foundation for GS_1 can be written as

$$q_{1Pasternak} = -k_w w_1 + k_G\left(\frac{\partial^2 w_1}{\partial x^2}+\frac{\partial^2 w_1}{\partial y^2}\right) \tag{23}$$

where k_w and k_G are Winkler's parameter and Pasternak's shear parameter of elastic medium, respectively.
The effective transverse load of van der Waals interaction for GS_1 is obtained as

$$q_{1vdW} = -k_0\left(w_1 - w_2\right) \tag{24}$$

Finally, the variation of work done by Lorentz magnetic force, Pasternak elastic foundation, van der Waals interaction and in-plane preload is calculated as

$$\delta V = -\int_{A}\Bigg[\left(q_{1magnetic}+q_{1Pasternak}+q_{1vdW}\right) - \left(N_{xx}^0\frac{\partial^2 w_1}{\partial x^2}+N_{yy}^0\frac{\partial^2 w_1}{\partial y^2}\right)\Bigg]\delta w_1 = \\ -\int_{A}\Bigg[\left(\eta hH_x^2\left(\frac{\partial^2 w_1}{\partial x^2}-\frac{\partial^2\phi_1}{\partial y^2}\right) - k_w w_1 + k_G\left(\frac{\partial^2 w_1}{\partial x^2}+\frac{\partial^2 w_1}{\partial y^2}\right) - k_0\left(w_1-w_2\right)\right) - \left(N_{xx}^0\frac{\partial^2 w_1}{\partial x^2}+N_{yy}^0\frac{\partial^2 w_1}{\partial y^2}\right)\Bigg]\delta w_1 \tag{25}$$

where N_{xx}^0 and N_{yy}^0 indicate in-plane preload forces exerting on the graphene sheet along *x* and *y* directions. The variation of kinetic energy can be written as

$$\delta K = \int_{V}\left(\dot{u}_{x1}\delta\dot{u}_{x1}+\dot{u}_{y1}\delta\dot{u}_{y1}+\dot{u}_{z1}\delta\dot{u}_{z1}\right)\rho dAdz = \int_{A}\left[\rho h\dot{w}_1\delta\dot{w}_1 + \frac{\rho h^3}{12}\left(\frac{\partial\dot{\phi}_1}{\partial x}\frac{\partial\delta\dot{\phi}_1}{\partial x}+\frac{\partial\dot{\phi}_1}{\partial y}\frac{\partial\delta\dot{\phi}_1}{\partial y}\right)\right]dA \tag{26}$$

Using the expressions for $\delta U, \delta V$ and δK from Eqs. (21), (25) and (26) in the preceding Eq. (19) and integrating the equation by parts, and setting the coefficients of, δu_1, $\delta v_1, \delta w_1$ and $\delta\theta_1$ to zero, the following equations of motion for GS_1 are obtained

$$\delta u_1 : \frac{\partial N_{xx1}}{\partial x}+\frac{\partial N_{xy1}}{\partial y} = \rho h\ddot{u}_1$$

$$\delta v_1 : \frac{\partial N_{xy1}}{\partial x}+\frac{\partial N_{yy1}}{\partial y} = \rho h\ddot{v}_1$$

$$\delta w_1 : \frac{\partial Q_{yz1}}{\partial y}+\frac{\partial Q_{zx1}}{\partial x}+\eta h H_x^2\left(\frac{\partial^2 w_1}{\partial x^2}-\frac{\partial^2 \phi_1}{\partial y^2}\right)-k_W w_1$$
$$+k_G\nabla^2 w_1-k_0(w_1-w_2)-N_{xx}^0\frac{\partial^2 w_1}{\partial x^2}-N_{yy}^0\frac{\partial^2 w_1}{\partial y^2}=\rho h\ddot{w}_1 \tag{27}$$
$$\delta\phi_1 : \frac{\partial^2 M_{xx1}}{\partial x^2}+2\frac{\partial^2 M_{xy1}}{\partial x\partial y}+\frac{\partial^2 M_{yy1}}{\partial y^2}-\frac{\partial Q_{yz1}}{\partial y}-\frac{\partial Q_{xz1}}{\partial x}=-\frac{\rho h^3}{12}\nabla^2\ddot{\phi}_1$$

For this case, the equations that correspond to the in-plane displacements $(\delta u_1, \delta v_1)$ are not coupled with the equations that correspond to the displacements due to bending. If we apply the operator $\Re = 1-(e_0\ell)^2\nabla^2$ to Eq. (27) and substitute Eqs. (16) and (17) into the resulting equation then equations of motion can be expressed via the displacement (w_1, ϕ_1)

$$H_{55}\left(\frac{\partial^2 w_1}{\partial x^2}-\frac{\partial^2 \phi_1}{\partial x^2}\right)+H_{44}\left(\frac{\partial^2 w_1}{\partial y^2}-\frac{\partial^2 \phi_1}{\partial y^2}\right)-k_W w_1+k_G\left(\frac{\partial^2 w_1}{\partial x^2}+\frac{\partial^2 w_1}{\partial y^2}\right)-k_0\left(w_1-w_2\right)+$$
$$-N_{xx}^0\frac{\partial^2 w_1}{\partial x^2}-N_{yy}^0\frac{\partial^2 w_1}{\partial y^2}+\eta h H_x^2\left(\frac{\partial^2 w_1}{\partial x^2}-\frac{\partial^2 \phi_1}{\partial y^2}\right)-\left(e_0\ell\right)^2\left[-k_W\left(\frac{\partial^2 w_1}{\partial x^2}+\frac{\partial^2 w_1}{\partial y^2}\right)+k_G\left(\frac{\partial^4 w_1}{\partial x^4}+2\frac{\partial^4 w_1}{\partial x^2\partial y^2}+\frac{\partial^4 w_1}{\partial y^4}\right)\right]$$
$$+\left(e_0\ell\right)^2 k_0\left(\frac{\partial^2 w_1}{\partial x^2}+\frac{\partial^2 w_1}{\partial y^2}-\frac{\partial^2 w_2}{\partial x^2}-\frac{\partial^2 w_2}{\partial y^2}\right)+\left(e_0\ell\right)^2 N_{xx}^0\left(\frac{\partial^4 w_1}{\partial x^4}+\frac{\partial^4 w_1}{\partial x^2\partial y^2}\right) \tag{28a}$$
$$+\left(e_0\ell\right)^2 N_{yy}^0\left(\frac{\partial^4 w_1}{\partial y^4}+\frac{\partial^4 w_1}{\partial x^2\partial y^2}\right)-\left(e_0\ell\right)^2\eta h H_x^2\left[\left(\frac{\partial^4 w_1}{\partial x^4}+\frac{\partial^4 w_1}{\partial x^2\partial y^2}\right)-\left(\frac{\partial^4 \phi_1}{\partial y^4}+\frac{\partial^4 \phi_1}{\partial x^2\partial y^2}\right)\right]=\rho h\ddot{w}_1$$
$$-\left(e_0\ell\right)^2\rho h\left(\frac{\partial^2 \ddot{w}_1}{\partial x^2}+\frac{\partial^2 \ddot{w}_1}{\partial y^2}\right)$$

$$D_{11}\frac{\partial^4 \phi_1}{\partial x^4}+2\left(D_{12}+2D_{66}\right)\frac{\partial^4 \phi_1}{\partial x^2\partial y^2}+D_{22}\frac{\partial^4 \phi_1}{\partial y^4}+H_{55}\left(\frac{\partial^2 w_1}{\partial x^2}-\frac{\partial^2 \phi_1}{\partial x^2}\right)+H_{44}\left(\frac{\partial^2 w_1}{\partial y^2}-\frac{\partial^2 \phi_1}{\partial y^2}\right)$$
$$=\frac{\rho h^3}{12}\left(\frac{\partial^2 \ddot{\phi}_1}{\partial x^2}+\frac{\partial^2 \ddot{\phi}_1}{\partial y^2}\right)-\left(e_0\ell\right)^2\frac{\rho h^3}{12}\left(\frac{\partial^4 \ddot{\phi}_1}{\partial x^4}+2\frac{\partial^4 \ddot{\phi}_1}{\partial x^2\partial y^2}+\frac{\partial^4 \ddot{\phi}_1}{\partial y^4}\right) \tag{28b}$$

Eqs. (28a) and (28b) are related to GS_1. In the same way the equations of motion for GS_2 are obtained.

$$H_{55}\left(\frac{\partial^2 w_2}{\partial x^2}-\frac{\partial^2 \phi_2}{\partial x^2}\right)+H_{44}\left(\frac{\partial^2 w_2}{\partial y^2}-\frac{\partial^2 \phi_2}{\partial y^2}\right)-k_W w_2+k_G\left(\frac{\partial^2 w_2}{\partial x^2}+\frac{\partial^2 w_2}{\partial y^2}\right)+k_0\left(w_1-w_2\right)+$$
$$-N_{xx}^0\frac{\partial^2 w_2}{\partial x^2}-N_{yy}^0\frac{\partial^2 w_2}{\partial y^2}+\eta h H_x^2\left(\frac{\partial^2 w_2}{\partial x^2}-\frac{\partial^2 \phi_2}{\partial y^2}\right)-\left(e_0\ell\right)^2\left[-k_W\left(\frac{\partial^2 w_2}{\partial x^2}+\frac{\partial^2 w_2}{\partial y^2}\right)+k_G\left(\frac{\partial^4 w_2}{\partial x^4}+2\frac{\partial^4 w_2}{\partial x^2\partial y^2}+\frac{\partial^4 w_2}{\partial y^4}\right)\right]$$
$$-\left(e_0\ell\right)^2 k_0\left(\frac{\partial^2 w_1}{\partial x^2}+\frac{\partial^2 w_1}{\partial y^2}-\frac{\partial^2 w_2}{\partial x^2}-\frac{\partial^2 w_2}{\partial y^2}\right)+\left(e_0\ell\right)^2 N_{xx}^0\left(\frac{\partial^4 w_2}{\partial x^4}+\frac{\partial^4 w_2}{\partial x^2\partial y^2}\right) \tag{28c}$$
$$+\left(e_0\ell\right)^2 N_{yy}^0\left(\frac{\partial^4 w_2}{\partial y^4}+\frac{\partial^4 w_2}{\partial x^2\partial y^2}\right)-\left(e_0\ell\right)\eta h H_x^2\left[\left(\frac{\partial^4 w_2}{\partial x^4}+\frac{\partial^4 w_2}{\partial x^2\partial y^2}\right)-\left(\frac{\partial^4 \phi_2}{\partial y^4}+\frac{\partial^4 \phi_2}{\partial x^2\partial y^2}\right)\right]=\rho h\ddot{w}_2$$
$$-\left(e_0\ell\right)^2\rho h\left(\frac{\partial^2 \ddot{w}_2}{\partial x^2}+\frac{\partial^2 \ddot{w}_2}{\partial y^2}\right)$$

$$D_{11}\frac{\partial^4 \phi_2}{\partial x^4}+2\left(D_{12}+2D_{66}\right)\frac{\partial^4 \phi_2}{\partial x^2\partial y^2}+D_{22}\frac{\partial^4 \phi_2}{\partial y^4}+H_{55}\left(\frac{\partial^2 w_2}{\partial x^2}-\frac{\partial^2 \phi_2}{\partial x^2}\right)+H_{44}\left(\frac{\partial^2 w_2}{\partial y^2}-\frac{\partial^2 \phi_2}{\partial y^2}\right)$$
$$=\frac{\rho h^3}{12}\left(\frac{\partial^2 \ddot{\phi}_2}{\partial x^2}+\frac{\partial^2 \ddot{\phi}_2}{\partial y^2}\right)-\left(e_0\ell\right)^2\frac{\rho h^3}{12}\left(\frac{\partial^4 \ddot{\phi}_2}{\partial x^4}+2\frac{\partial^4 \ddot{\phi}_2}{\partial x^2\partial y^2}+\frac{\partial^4 \ddot{\phi}_2}{\partial y^4}\right) \tag{28d}$$

The equations (28) present the equations of motion for orthotropic DLGSs.

III. Solution by Galerkin's method

In this section, the equations of motion (28) are solved analytically using Galerkin's method to obtain the vibrational frequencies of the DLGSs subjected to in-plane preload. Before solving the equations of motion, the boundary conditions should be defined. In this study the graphene sheet is assumed to have simply supported (S), clamped (C) edges or have combinations of them. These boundary conditions are given as follows[43,26]:

Simply supported (S):

$$u_i = \frac{\partial \phi_i}{\partial y} = w_i = M_{xxi} = 0, \qquad \text{at } x = 0, \mathrm{a}$$

$$v_i = \frac{\partial \phi_i}{\partial x} = w_i = M_{yyi} = 0, \qquad \text{at } y = 0, b \text{ ; } i=1,2; \tag{29}$$

Clamped (C):

$$u_i = \frac{\partial \phi_i}{\partial x} = \frac{\partial \phi_i}{\partial y} = w_i = 0, \qquad \text{at } x = 0, \mathrm{a}$$

$$v_i = \frac{\partial \phi_i}{\partial x} = \frac{\partial \phi_i}{\partial y} = w_i = 0, \qquad \text{at } y = 0, b \text{ ; } i=1,2; \tag{30}$$

To satisfy the above boundary conditions, the displacement quantities can be written in the following form:

$$\begin{aligned} w_1(x,y) &= W_{1mn} X(x) Y(y) e^{i\omega t} \\ \phi_1(x,y) &= \phi_{1mn} X(x) Y(y) e^{i\omega t} \\ w_2(x,y) &= W_{2mn} X(x) Y(y) e^{i\omega t} \\ \phi_2(x,y) &= \phi_{2mn} X(x) Y(y) e^{i\omega t} \end{aligned} \tag{31}$$

where $i = \sqrt{-1}$, $(W_{1mn}, \phi_{1mn}, W_{2mn}, \phi_{2mn})$ are arbitrary parameters, $\omega = \omega_{mn}$ denotes vibrational frequency associated with (mth, nth) mode, m and n are half wave numbers, and the functions $X(x)$ and $Y(y)$ satisfies the simply supported and clamped boundary conditions and therefore it is given in Table 1, where $\alpha = m\pi / \mathrm{a}, \beta = n\pi / b$. These functions are suggested in Refs.[43,25,26]. The method of marking the boundary conditions has been explained in Table 1. For example, the symbol CSCS, identifies a graphene sheet with the edges $x = 0, \mathrm{a}$ are clamped (C), while the edges $y = 0, b$ are simply supported (S).

Table no 1: The admissible functions *X(x)* and *Y(y)*

Boundary conditions					The functions X(x) and Y(y)	
Notation	x=0	y=0	x= a	y= b	X(x)	Y(y)
SSSS	S	S	S	S	$\sin(\alpha x)$	$\sin(\beta y)$
SCSC	S	C	S	C	$\sin(\alpha x)$	$\sin^2(\beta y)$
CCCC	C	C	C	C	$\sin^2(\alpha x)$	$\sin^2(\beta y)$
CSCS	C	S	C	S	$\sin^2(\alpha x)$	$\sin(\beta y)$

Substituting Eq. (31) into Eq. (28) and applying Galerkin's method, the analytical solution of the equations of motion in terms of parameters W_{1mn}, ϕ_{1mn}, W_{2mn} and ϕ_{2mn} can be obtained from

$$\left(\begin{bmatrix} K_{11} & K_{12} & K_{13} & 0 \\ K_{21} & K_{22} & 0 & 0 \\ K_{31} & 0 & K_{33} & K_{34} \\ 0 & 0 & K_{43} & K_{44} \end{bmatrix} - \omega^2 \begin{bmatrix} m_{11} & 0 & 0 & 0 \\ 0 & m_{22} & 0 & 0 \\ 0 & 0 & m_{33} & 0 \\ 0 & 0 & 0 & m_{44} \end{bmatrix} \right) \begin{Bmatrix} W_{1mn} \\ \phi_{1mn} \\ W_{2mn} \\ \phi_{2mn} \end{Bmatrix} = \begin{Bmatrix} 0 \\ 0 \\ 0 \\ 0 \end{Bmatrix} \tag{32}$$

where

$$
\begin{aligned}
&K_{11} = \left(H_{55} - N_{xx}^0 + k_G + \mu^2 k_w + \mu^2 k_0 + \eta h H_x^2\right)\gamma_1 + \left(H_{44} - N_{yy}^0 + k_G + \mu^2 k_w + \mu^2 k_0\right)\gamma_2 \\
&-\left(k_w + k_0\right)\gamma_4 - \mu^2\left(k_G - N_{xx}^0 + \eta h H_x^2\right)\gamma_3 - \mu^2\left(k_G - N_{yy}^0\right)\gamma_5 - \mu^2\left(2k_G - N_{xx}^0 - N_{yy}^0 + \eta h H_x^2\right)\gamma_6 \\
&K_{12} = -H_{55}\gamma_1 - \left(H_{44} + \eta h H_x^2\right)\gamma_2 + \mu^2 \eta h H_x^2\left(\gamma_5 + \gamma_6\right) \\
&K_{13} = k_0\gamma_4 - \mu^2 k_0\left(\gamma_1 + \gamma_2\right) \\
&K_{22} = -H_{55}\gamma_1 - H_{44}\gamma_2 + D_{11}\gamma_3 + 2\left(D_{12} + 2D_{66}\right)\gamma_6 + D_{22}\gamma_5 \\
&K_{21} = H_{55}\gamma_1 + H_{44}\gamma_2, \\
&K_{31} = K_{13},\ K_{33} = K_{11},\ K_{34} = K_{12},\ K_{43} = K_{21},\ K_{44} = K_{22} \\
&m_{11} = -\rho h\gamma_4 + \mu^2 \rho h\left(\gamma_1 + \gamma_2\right) \\
&m_{22} = \frac{-\rho h^3}{12}\left(\gamma_1 + \gamma_2\right) + \mu^2 \frac{\rho h^3}{12}\left(\gamma_3 + 2\gamma_6 + \gamma_5\right) \\
&m_{33} = m_{11},\ \ m_{44} = m_{22}
\end{aligned}
\tag{33}
$$

$$
\begin{aligned}
&\gamma_1 = \int_0^a\int_0^b X''XY^2 dxdy,\ \ \gamma_2 = \int_0^a\int_0^b Y''YX^2 dxdy, \\
&\gamma_3 = \int_0^a\int_0^b X''''XY^2 dxdy,\ \gamma_4 = \int_0^a\int_0^b X^2Y^2 dxdy, \\
&\gamma_5 = \int_0^a\int_0^b Y''''YX^2 dxdy,\ \ \gamma_6 = \int_0^a\int_0^b X''XY''Ydxdy
\end{aligned}
\tag{34}
$$

In Eq. (33) the mark for nonlocal parameter $\mu = e_0\ell$ has been used. By solving Eq. (32) the analytical solutions for the vibrational frequency are obtained for two characteristics of the vibration cases.

Out-of-phase vibration

In this case, two graphene sheets vibration asynchronously and it means that there is a relative displacement between them $\left(w_1 \neq w_2\right)$. The first solution Eq. (32) gives the value for the vibrational frequency for out-of-phase vibration

$$
\omega_{out} = \sqrt{\frac{-A_4 + \sqrt{A_4^2 - 4A_1A_5}}{2A_1}} \tag{35}
$$

where

$$
\begin{aligned}
&A_1 = \frac{\rho^2 h^4}{12}\left(\gamma_4 - \mu^2\delta_1\right)\left(\delta_1 - \mu^2\delta_2\right) \\
&A_4 = \rho h\left(\gamma_4 - \mu^2\delta_1\right)\left(B_3 - B_2\right) + \frac{\rho h^3}{12}\left(\delta_1 - \mu^2\delta_2\right)\left[P_3 + 2k_0\left(\mu^2\delta_1 - \gamma_4\right)\right] \\
&A_5 = P_3\left(B_3 - B_2\right) - B_2\left(B_4 - B_2\right) + 2k_0\left(\mu^2\delta_1 - \gamma_4\right)\left(B_3 - B_2\right) \\
&P_1 = k_w(\mu^2\delta_1 - \gamma_4) + k_G(\delta_1 - \mu^2\delta_2) + \eta h H_x^2\left[\gamma_1 - \mu^2(\gamma_3 + \gamma_6)\right] \\
&\delta_1 = \gamma_1 + \gamma_2 \\
&\delta_2 = \gamma_3 + 2\gamma_6 + \gamma_5 \\
&B_2 = H_{55}\gamma_1 + H_{44}\gamma_2 \\
&B_3 = D_{11}\gamma_3 + 2(D_{12} + 2D_{66})\gamma_6 + D_{22}\gamma_5 \\
&B_4 = \eta h H_x^2\left[\mu^2\left(\gamma_5 + \gamma_6\right) - \gamma_2\right] \\
&P_3 = P_1 + B_2 - N\left(\gamma_1 + k\gamma_2\right) \\
&N_{xx}^0 = N,\ \ N_{yy}^0 = kN
\end{aligned}
\tag{36}
$$

In-phase vibration

In the case of in-phase vibration, two graphene sheets vibrate synchronously and it means that there is no relative displacement between them $(w_1 = w_2)$.Using the Galerkin's method the second solution of Eq. (32) gives the vibrational frequency for in-phase vibration

$$\omega_{in} = \sqrt{\frac{-A_2 + \sqrt{A_2^2 - 4A_1A_3}}{2A_1}} \tag{37}$$

where

$$A_4 = \rho h\left(\gamma_4 - \mu^2\delta_1\right)\left(B_3 - B_2\right) + \frac{\rho h^3}{12}\left(\delta_1 - \mu^2\delta_2\right)P_3$$
$$A_5 = P_3\left(B_3 - B_2\right) - B_2\left(B_4 - B_2\right) \tag{38}$$

IV. Numerical results and discussions

In this section, the effect of unidirectional magnetic field strength, nonlocal parameter, number of half waves, initial preload, size of nanoplate and boundary conditions on vibrational frequency is investigated. The material and geometrical properties of the orthotropic graphene sheet are adopted from papers[44,45,26] as follows: Young's modulus $E_1 = 1130\,GPa$ and $E_2 = 1050\,GPa$ of the orthotropic graphene sheet, mass density $\rho = 2250\,kg/m^3$, Poisson's ratio $\nu_{12} = 0.112$ and $\nu_{21} = 0.0803$, shear modulus $G_{12} = E_1/2\left(1+\nu_{12}\right) = 508.09\,GPa$ and $G_{13} = G_{23} = \frac{5}{6}G_{12} = 423.41\,GPa$, thickness of graphene sheet $h = 0.34\,nm$.

In the present study we have used the value for the magnetic field strength in the range $H_x = 0 \div 0.1251\,A/nm$ and in the case of a square nanoplate with the dimensions $10\,nm$ it corresponds to the value of dimensionless magnetic parameter ($MP = \eta h H_x^2\,\mathrm{a}^2/D_{11}$) within the limits $0 \div 180$. In Ref.[46] the value for dimensionless magnetic parameter has been taken in the range of $0 \div 100$, and in Ref. [39] in the range of $0 \div 160$. Also, in the present study, we have used the values $k_0 = 0.15\ GPa/nm,\ k_w = 0.075\ GPa/nm,\ k_G = 0.75\ N/m$, as in Ref.[26].

In the comparison study the following dimensionless parameters are used:

$$\omega_{N1} = \omega^2\,\mathrm{a}^2\sqrt{\frac{\rho h}{D_{11}}},\ \omega_{N2} = \frac{\omega^2\,\mathrm{a}^2}{\pi^2}\sqrt{\frac{\rho h}{D_{11}}},\ k_{wN} = \frac{k_w\,\mathrm{a}^4}{D_{11}},\ k_{GN} = \frac{k_G\,\mathrm{a}^2}{D_{11}},\ k_{0N} = \frac{k_0\,\mathrm{a}^4}{D_{11}}$$
$$MP = \frac{\eta h H_x^2\,\mathrm{a}^2}{D_{11}}$$

Verification of the predict results with those of another work

In the first example of validation, the present results for the dimensionless frequency (ω_{N1}) of isotropic rectangular single-layer graphene sheet with a simply supported boundary conditions subjected to in-plane magnetic field are compared to the results of Kiani[46] in Table 2. The material properties and geometrical characteristics applied in this analysis are defined as: $E = 1060\,GPa,\ \nu = 0.25,\ \rho = 2250\,kg/m^3, k_{WN} = 100,\ k_{GN} = 0,\ \mu = 1.345\,nm,\ \mathrm{a} = 10\,nm, b = 15\,nm, h = 0.34\,nm.$ As shown in Table 2 the present results for dimensionless frequency are in excellent agreement with the results presented by Ref.[46].

Table no 2: Comparison of the present dimensionless frequencies (ω_{N1}) with that in literature for square SLGSs subjected to magnetic field obtained from nonlocal Classical Plate Theory

MP	Kiani[46]	Present
0	16,1731	16,1359
10	17,7876	17,7582
20	19,2442	19,2673

30	20,6234	20,6413
40	21,9160	21,9293
50	23,1364	23,1457
60	24,2957	24,3013
70	25,4020	25,4045
80	26,4622	26,4616
90	27,4815	27,4781
100	28,4643	28,4584

In the second example, dimensionless frequency (ω_{N2}) of isotropic plates with CCCC and CSCS boundary conditions is examined. The material properties and geometrical characteristics applied in this analysis are defined as: $E = 210\ GPa$, $\nu = 0.3$, a/*b=1, h*/a=*0.1.* As a result, by ignoring the terms related to the size effect $(\mu = 0)$, the dimensionless frequencies at macroscale obtained via classical NFSDT are calculated and compared with those reported by[47,48,35]. As indicated in Table 3, a strong agreement is found between the present results and the results in Ref.[47,48,35].

Table no 3: Comparison of the present dimensionless fundamental frequencies (ω_{N2}) with that in literature for square SLGSs.

CCCC				CSCS	
Zhang [35]	Reddy [47]	Bardell [48]	Present	Bardell [48]	Present
3,619	3,648	3,646	3,734	2,741	2,827

Parametric study

In this section, the effects of the nonlocal parameter, magnetic field strength, in-plane preload (compression and tension), various boundary conditions, aspect ratio, side length and number of half waves on the vibrational behaviour of DLGSs are discussed in detail.

In Fig. 2 (a), (b) and (c) the in-phase natural frequency for SSSS boundary conditions is plotted as a function of the nonlocal parameter for various values of the magnetic field strength. From Fig. 2 (a) and (c) it can be noticed easily that in the case of a square DLGS $(a = b = 10\,nm)$ and an equal number of half waves $(m = n = 1, m = n = 2)$ with the increase of value of the magnetic field strength the increase of value of the natural frequency is negligibly low. In the case when the number of half waves is $(m = 2, n = 1)$ the increase of value of the natural frequency is significant with the increase of value of the magnetic field strength.

Figure no 2: Change in in-phase fundamental frequency with respect to nonlocal parameter and magnetic field strength for SSSS boundary conditions

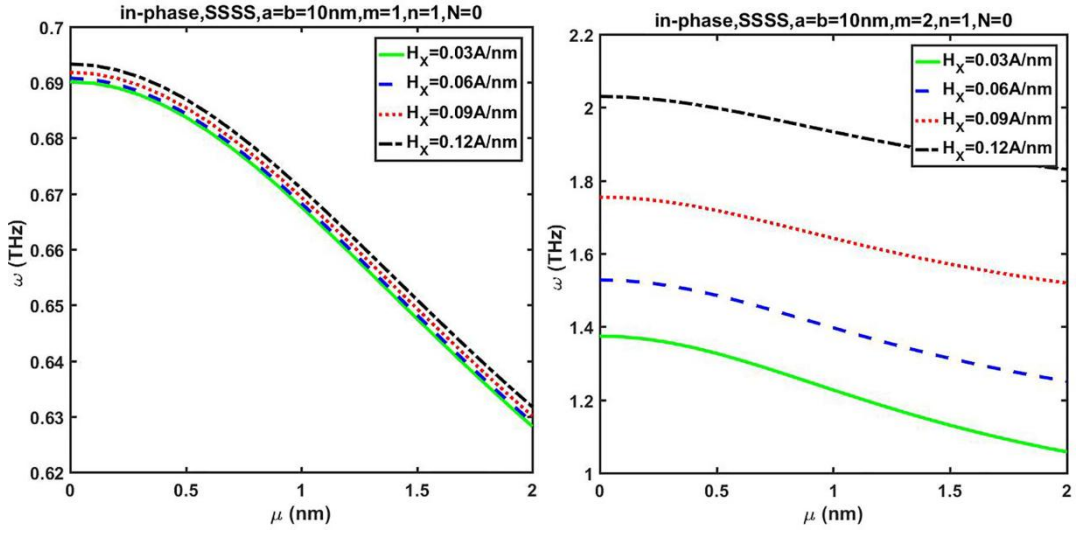

(a) (b)

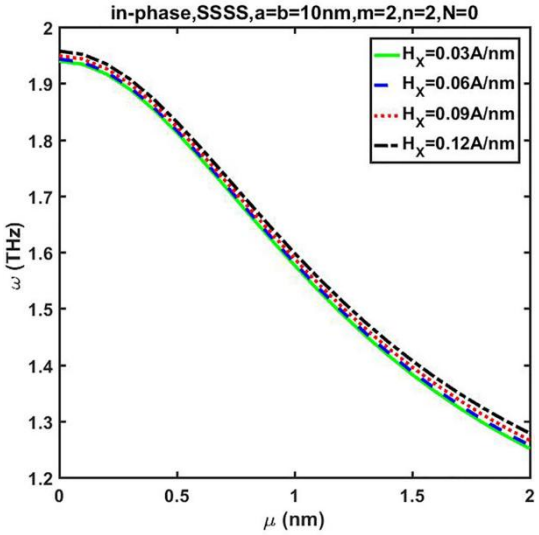

(c)

From Fig. 3 (a), (b) and (c) it can be seen that in the case of out-of-phase vibration the behaviour of a square DLGS (a = b = 10 nm) with the change of value of magnetic field strength and number of half waves is the same as in the case of in-phase vibration.

Figure no 3: Change in out-of-phase fundamental frequency with respect to nonlocal parameter and magnetic field strength for SSSS boundary conditions

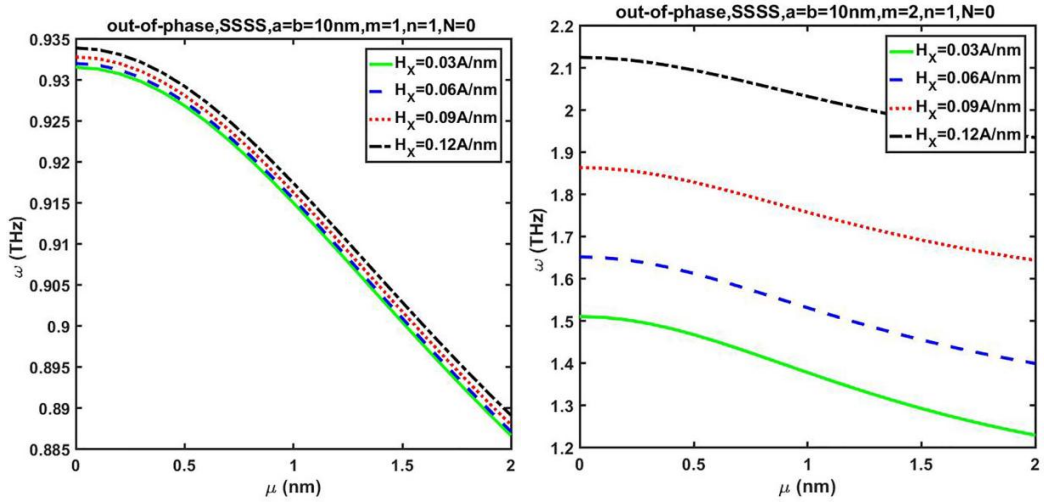

(a)

(b)

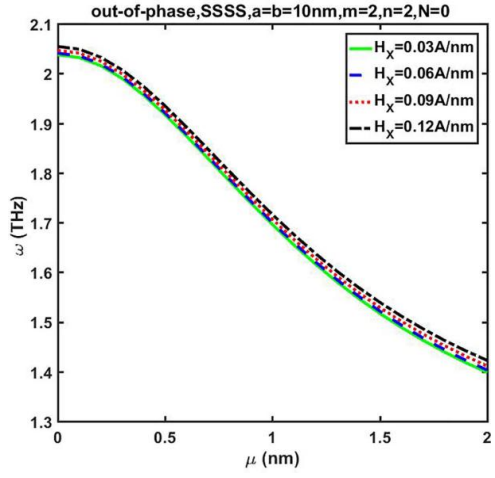

(c)

Fig. 4(a), (b) and (c) demonstrates in-phase natural frequency versus nonlocal parameter for different values of magnetic field strength and CCCC boundary conditions. In the case of a square DLGS $(a = b = 10\,nm)$ and equal number of half waves $(m = n = 1, m = n = 2)$ with the increase of value of the magnetic field strength the change in the value the natural frequency does not occur. It can be concluded that in these cases the in-plane magnetic field does not affect the vibrational behaviour of DLGS. In the case when the number of half waves is $(m = 2, n = 1)$ with the increase of value of magnetic field strength the value of the natural frequency (Fig. 4b) also increases. From Fig. 4b it can be noticed that in the case of CCCC boundary conditions the increase of value of magnetic field strength decreases the nonlocal effect, and that is not the case in SSSS boundary conditions.

Figure no 4: Change in in-phase fundamental frequency with respect to nonlocal parameter and magnetic field strength for CCCC boundary conditions

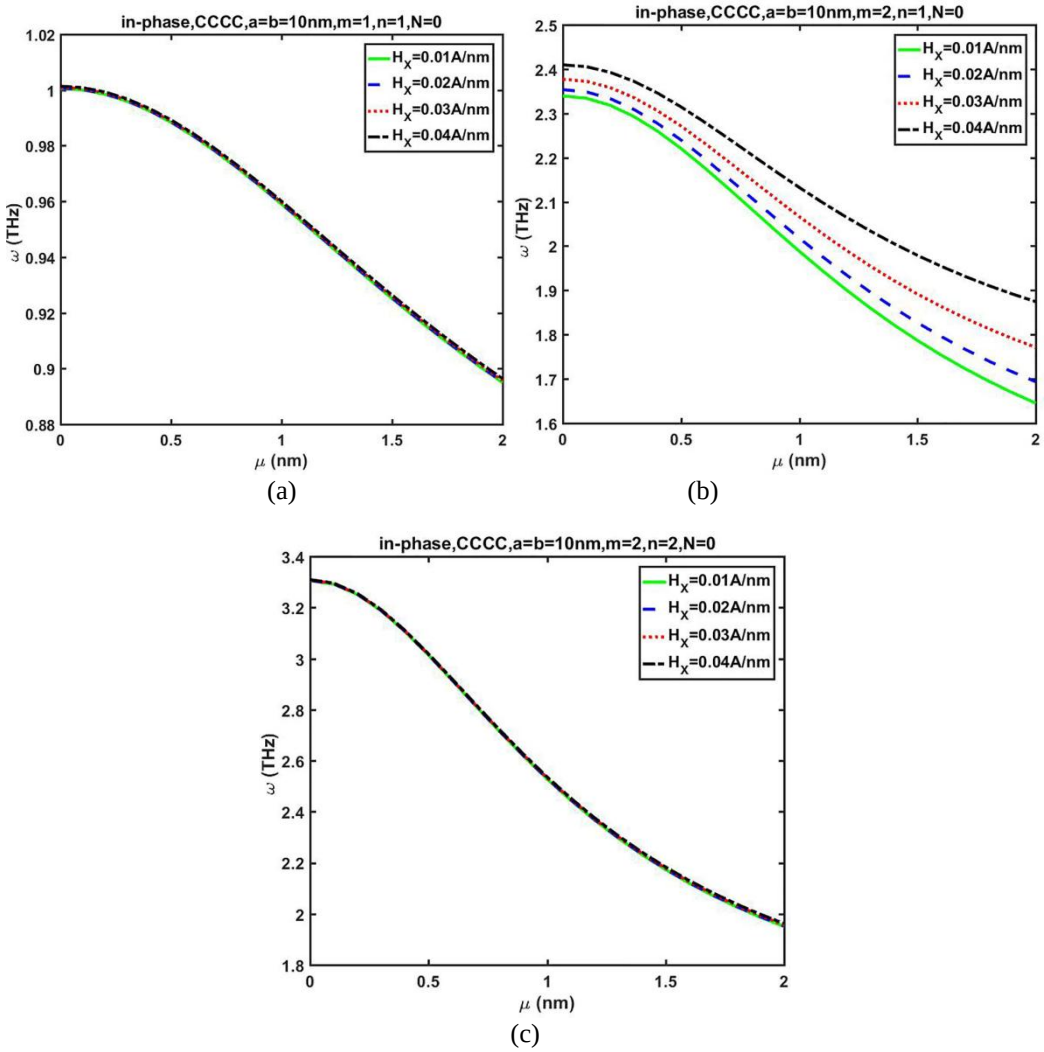

From Fig. 5 (a), (b) and (c) it can be seen that in the case of out-of-phase vibration for CCCC boundary conditions the behaviour of a square DLGS $(a = b = 10\,nm)$ with the change of value of magnetic field strength and number of half waves is similar as in the case of in-phase vibration. From Fig. 5(b) it can be observed that in the case when the number of number of half waves is $(m = 3, n = 1)$ with the increase of value of magnetic field strength the influence of local effect to the value of the natural frequency decreases significantly.

Figure no 5: Change in out-of-phase fundamental frequency with respect to nonlocal parameter and magnetic field strength for CCCC boundary conditions

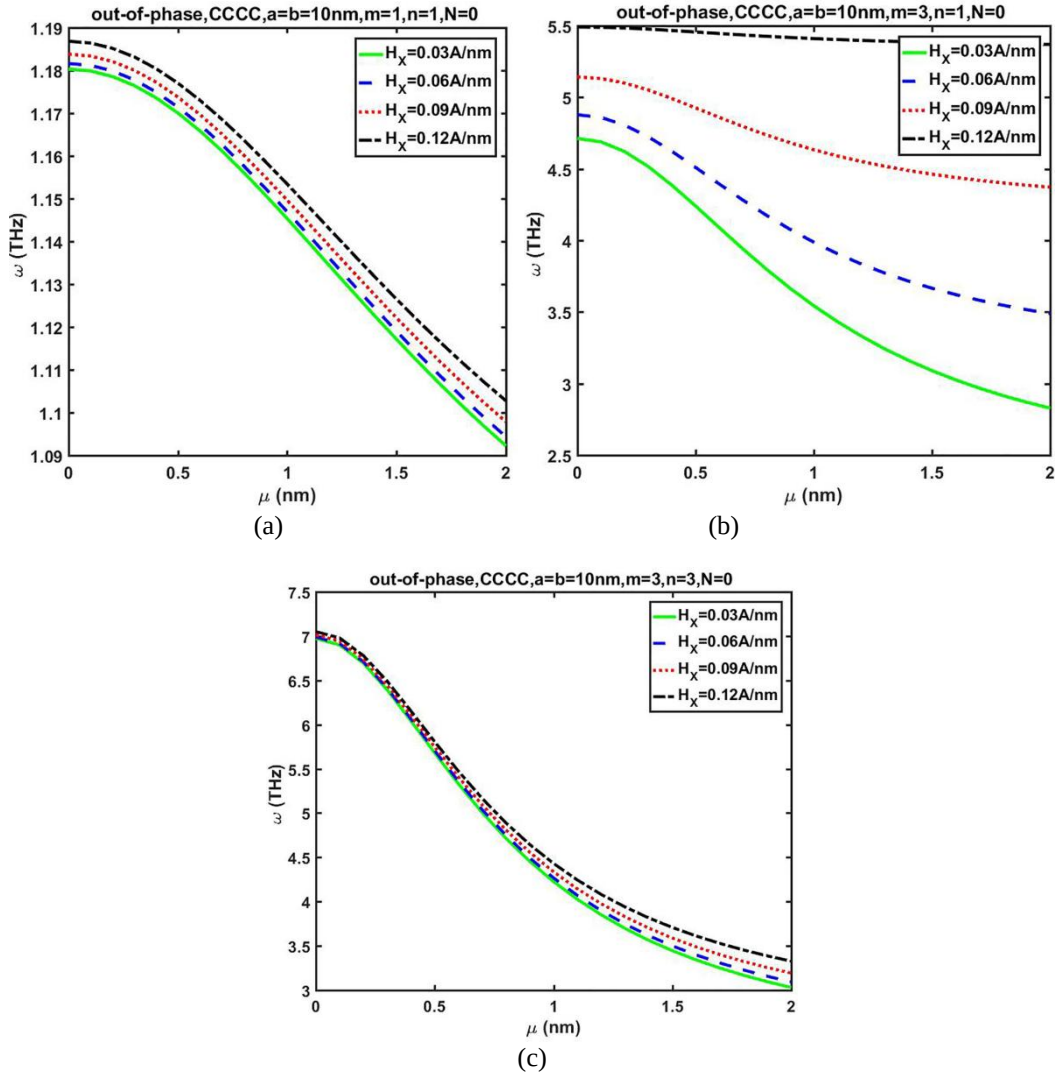

Fig.6 (a) and (b) provides the variations of the in-phase natural frequency for various amounts of nonlocal parameter for CSCS and SCSC boundary conditions, respectively. In both cases, a square DLGS (a=b=10 nm) is observed with numbers of half waves (m=1, n=1). It is obvious that in the case of CSCS boundary conditions with the increase of value of magnetic field strength the increase of value of the natural frequency occurs. In the case of SCSC boundary conditions, the situation is reverse, so that with the increase of value of the magnetic field strength a decrease of value of the natural frequency occurs. In the case of CSCS boundary conditions with the increase of value of magnetic field strength the influence of nonlocal effect is decreased, while in the case of SCSC boundary conditions it is increased.

Figure no 6: Change in in-phase fundamental frequency with respect to nonlocal parameter and magnetic field strength for CSCS and SCSC boundary conditions

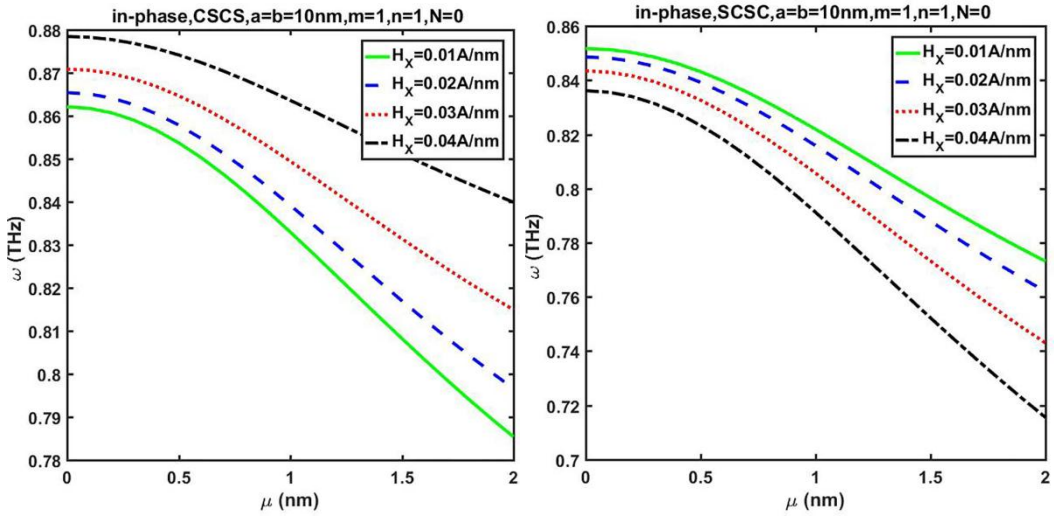

(a) (b)

From Fig. 7(a) and (b) it can be noticed that in the case out-of-phase vibration we have an identical behaviour as in the case of in-phase vibration for CSCS and SCSC boundary conditions

Figure no 7: Change in out-of-phase fundamental frequency with respect to nonlocal parameter and magnetic field strength for CSCS and SCSC boundary conditions.

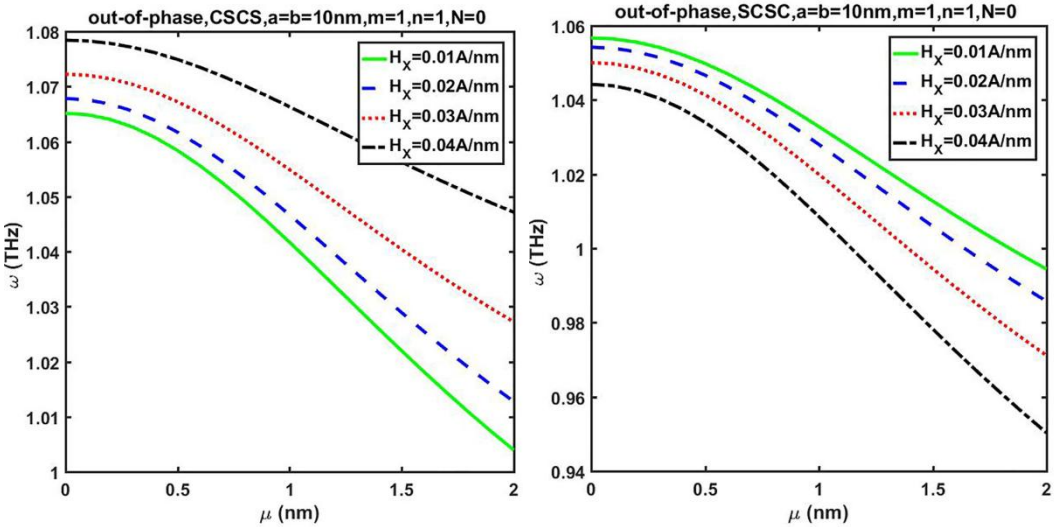

(a) (b)

V. Conclusions

In this paper, in-phase and out-of-phase vibration of the orthotropic double-nanoplate system subjected to unidirectional in-plane magnetic field and initial in-plane (compression and tension) preload with various boundary conditions was presented. By using Hamilton's principle, the equations of motion and boundary conditions were obtained base on the new first order shear deformation theory in the framework of the Eringen's differential nonlocal elastic law. The Galerkin's method has been used to solve the equations of motion of the DLGS for SSSS, CCCC, CSCS and SCSC boundary conditions. The present analytical solution is validated by comparing results with results available in the literature. Numerical results are presented to investigate the effects of nonlocal parameter, magnetic field strength, number of half waves and boundary conditions on vibrational frequency. It is observed that increasing the nonlocal parameter will decrease the frequency and increasing the in-plane compression preload degrades the graphene sheet stiffness and frequency reduce until a critical point in which frequency becomes zero. Also, the frequency increase with the increase of the magnetic field strength for rectangular DLGS.

References

[1]. Murmu T, Adhikari S. Nonlocal mass nanosensors based on vibrating monolayer graphene sheets. Sensors and Actuators B: Chemical 2013;188:1319-1327.
[2]. Roy S, Gao Z. Nanostructure-based electrical biosensors. Nano Today 2009;4:318-334.
[3]. Chang T, Sun X. Analysis and control of monolithic piezoelectric nano-actuator. IEEE Transactions on Control Systems Technology 2001;9:69-75.
[4]. Eichler A, Moser J, Chaste J, Zdrojek M, Wilson-Rae I, Bachtold A. Nonlinear damping in mechanical resonators made from carbon nanotubes and graphene. Nature Nanotechnology 2011;6:339-342.
[5]. Behfar K, Naghdabadi R. Nanoscale vibrational analysis of a multi-layered graphene sheet embedded in an elastic medium. Composites Science and Technology 2005;65:1159-1164.
[6]. He XQ, Kitipornchai S, Liew KM. Resonance analysis of multi-layered graphene sheets as nanoscale resonators. Nanotechnology 2005;16:2086-2091.
[7]. Kitipornchai S, He XQ, Liew KM. Continuum model for the vibration of multi-layered graphene sheets. Physical Review B 2005;72:075443.
[8]. Liew KM, He XQ, Kitipornchai S. Predicting nanovibration of multi-layered graphene sheets embedded in an elastic matrix. Acta Materialia 2006;54:4229-4236.
[9]. Arash B, Wang Q. Vibration of single- and double-layered graphene sheets. Journal of Nanotechnology in Engineering and Medicine 2011;2:011012.
[10]. Eringen AC, Edelen DGB. On nonlocal elasticity. International Journal of Engineering Science 1972;10:233-248.
[11]. Eringen AC. On differential equations of nonlocal elasticity and solutions of screw dislocation and surface waves. Journal of Applied Physics 1983;54:4703-4710.
[12]. Reddy JN. Nonlocal theories for bending, buckling and vibrations of beam. International Journal of Engineering Science 2007;45:288-307.
[13]. Pradhan SC, Phadikar JK. Nonlocal elasticity theory for vibration of nanoplates. Journal of Sound and Vibration 2009;325:206-223.
[14]. Mindlin R. Second gradient of strain and surface-tension in linear elasticity. International Journal of Solides and Structures 1965;1:414-438.
[15]. Kong S, Zhou S, Nie Z, Wang K. Static and dynamic analysis of micro beams based on strain gradient elasticity theory. International Journal of Engineering Science 2009;47:487-498.
[16]. Koiter WT. Couple- stress in the theory of elasticity: I and II. Royal Netherlands Academy of Arts and Sciences 1964;67:17-44.
[17]. Agköz B, Civalek Ö. Free vibration analysis for single-layered graphene sheets in an elastic matrix via modified couple stress theory. Materials and Design 2012;42:164-171.
[18]. Pradhan SC, Kumar A. Vibration analysis of orthotropic graphene sheets using nonlocal elasticity theory and differential quadrature method. Composites Structures 2011;93:774-779.
[19]. Murmu T, Pradhan SC. Vibration analysis of nanoplates unde uniaxial prestressed conditions via nonlocal elasticity. Journal of Applied Physics 2009;106:104301.
[20]. Kiani K. Vibration analysis of elastically restrained double-walled carbon nanotubes on elastic foundation subjected to axial load using nonlocal shear deformable theories. International Journal of Mechanical Sciences 2012;68:16-34.
[21]. Mohammadi M, Goodarzi M, Ghayour M, Farajpour A. Influence of in-plane pre-load on the vibration frequency of circular graphene sheet via nonlocal continuum theory. Composites Part B 2013;51:121-129.
[22]. Asemi SR, Farajpour HR, Asemi M, Mohammadi M. Influence of initial stress on the vibration of double-piezoelectric-nanoplate systems with various boundary conditions using DQM. Physica E 2014;63:169-179.
[23]. Mohammadimehr M, Navi BR, Arani AG. Free vibration of viscoelastic double-bonded polymeric nanocomposite plates reinforced by FG-SWCNTs using MSGT, sinusoidal shear deformation theory and meshless method. Composite Structures 2015;131:654-671.
[24]. Liu JC, Zhang YQ, Fan LF. Nonlocal vibration and biaxial buckling of double-viscoelastic-FGM- nanoplate system with viscoelastic Pasternak medium in between. Physics Letters A 2017;381:1228-1235.
[25]. Radić N, Jeremić D. Thermal buckling of double-layered graphene sheets embedded in an elastic medium with various boundary conditions using nonlocal new first-order shear deformation theory. Composites Part B 2016;97:201-215.
[26]. Radić N, Jeremić D. A comprehensive study on vibration and buckling of orthotropic double-layered graphene sheets under hygrothermal loading with different boundary conditions. Composites Part B 2017;128:182-199.
[27]. Güven U. Transverse vibrations of single-walled carbon nanotubes with initial stress under magnetic field. Composite Structures 2014;114:92-98.
[28]. Kiani K. Characterization of free vibration of elastically supported double-walled carbon nanotubes subjected to a longitudinally varying magnetic field. Acta Mechanica 2013;224:3139-3151.
[29]. Murmu T, McCarthy MA, Adhikari S. Vibration response of double-walled carbon nanotubes subjected to an externally applied longitudinal magnetic field: A nonlocal elasticity approach. Journal of Sound and Vibration 2012;331:5069-5086.
[30]. Kiani K. Vibration and instability of a single-walled carbon nanotube in a three-dimensional magnetic field. Journal of Physics and Chemistry of Solids 2014;75:15-22.
[31]. Murmu T, McCarthy MA, Adhikari S. In-plane magnetic fields affected transverse vibration of embedded single-layer graphene sheets using equivalent nonlocal elasticity approach. Composite Structures 2013;96:57-63.
[32]. Kiani K. Free vibration of conducting nanoplates exposed to unidirectional in-plane magnetic fields using nonlocal shear deformable plate theories. Physica E 2014;57:179-192.
[33]. Ghorbanpour Arani AH, Maboudi MJ, Ghorbanpour Arani A, Amir S. 2D Magnetic field and biaxial in-plane pre-load effects on the vibration on double bonded orthotropic graphene sheets. Journal of Solids Mechanics 2013;5:193-205.
[34]. Ghorbanpour Arani A, Haghparast E, BabaAkbar Zarei H. Nonlocal vibration of axially moving graphene sheet resting on orthotropic visco-Pasternak foundation under longitudinal magnetic field. Physica B 2016;495:35-49.
[35]. Zhang Y, Zhang LW, Liew KM, Yu JL. Free vibration analysis of bilayer graphene sheets subjected to in-plane magnetic fields. Composite Structures 2016;144:86-95.
[36]. Karličić D, Cajić M, Adhikari S, Kozić P, Murmu T. Vibrating nonlocal multi-nanoplate system under inplane magnetic field. European Journal of Mechanics A/Solids 2017;64:29-45.
[37]. Stamenković Atanasov M, Karličić D, Kozić P. Forced transverse vibrations of an elastically connected nonlocal orthotropic double-nanoplate system subjected to an in-plane magnetic field. Acta Mechanica 2017;228:2165-2185.
[38]. Satish N, Narendar S, Brahma Raju K. Magnetic field and surface elasticity effects on thermal vibration properties of nanoplates. Composite Structures 2017;180:568-580.

[39]. Jamalpoor A, Hosseini M. Biaxial buckling analysis of double-orthotropic micro-plate-systems including in-plane magnetic field based on strain gradient theory. Composites Part B 2015;75:53-64.
[40]. Ebrahimi F, Reza Barati M. Vibration analysis of graphene sheets resting on orthotropic elastic medium subjected to hygro-thermal and in-plane magnetic fields based on the nonlocal strain gradient theory. Journal of Mechanical Engineering Science 2017; doi: 10.1177/0954406217720232.
[41]. Shimpi RP, Patel HG, Arya H. New first-order shear deformation theory. Jornal of Applied Mechanics 2007;47:523-533.
[42]. Xiang W, Xing Y. A new first-order shear deformation theory for free vibrations of rectangular plate. International Journal of Applied Mechanics 2015;7:1550008.
[43]. Thai HT, Nguyen TK, Vo TP, Lee J. Analysis of functionally graded sandwich plate using a new first-order shear deformation theory. European Journal of Mechanics-A/Solids 2014;45:211-225.
[44]. Ni Z, Bu H, Zou M, Yi H, Bi K, Chen Y. Anisotropic mechanical properties of graphene sheets from molecular dynamics. Physica B 2010;405:1301-1306.
[45]. Hosseini Kordkheili SA, Moshrefzadeh-Sani H. Mechanical properties of double-layered graphene sheets. Computational Materials Science 2013;69:335-343.
[46]. Kiani K. Revisiting the free transverse vibration of embedded single-layer graphene sheets acted upon by an in-plane magnetic field. Journal of Mechanical Science and Technology 2014;28:3511-3516.
[47]. Krishna Reddy AR, Palaninathan R. Free vibrations of skew laminates. Computers and Structures 1999;70:415-423.
[48]. Bardell NS. The free vibration of skew plates using the hierarchical finite element method. Computers and Structures 1992;45:841-874.

Nebojša Radić "Vibration analysis of orthotropic double-nanoplate system subjected to unidirectional in-plane magnetic field with various boundary conditions." IOSR Journal of Mechanical and Civil Engineering (IOSR-JMCE) , vol. 15, no. 3, 2018, pp. 59-76.